High-Quality ZnO Nanowire Arrays Directly Fabricated from Photoresists

Chun Cheng,[†] Ming Lei,[†] Lin Feng,[†] Tai Lun Wong,[†] K. M. Ho,[†] Kwok Kwong Fung,[†] Michael M. T. Loy,[†] Dapeng Yu,[‡] and Ning Wang[†,*]

[†]Department of Physics and the Institute of Nano Science and Technology, the Hong Kong University of Science and Technology, Hong Kong, China, and [‡]Department of Physics, Peking University, Beijing, P.R. China

ABSTRACT We report a simple and effective method for fabricating and patterning high-quality ZnO nanowire arrays using carbonized photoresists to control the nucleation site, density, and growth direction of the nanowires. The ZnO nanowires fabricated using this method show excellent alignment, crystal quality, and optical properties that are independent of the substrates. The carbonized photoresists provide perfect nucleation sites for the growth of aligned ZnO nanowires and they also perfectly connect to the nanowires to form ideal electrodes that can be used in many applications of ZnO nanomaterials.

KEYWORDS: zinc oxide · nanowire array · pattern · photoresist · antireflection · graphite

ZnO nanoscale materials, such as nanowires, have received increasing attention over the past few years because of their exciting potential applications in optoelectronic devices,[1] sensors,[2] highly efficient photonic devices,[3] near-UV lasers,[4] nanogenerators,[5] antireflection coatings (ARCs),[6] and electrochromic displays,[7] *etc*. Traditionally, patterned and aligned nanowires can be fabricated by patterning metal catalytic particles, often gold, on lattice-matching substrates through vapor−liquid−solid (VLS) growth, although this growth strategy involves tedious lift-off processes for patterning metal catalysts[2,4,5,8] and may lead to serious contamination in complementary metal oxide semiconductor processing.[9,10] There have been some reports on the use of nongold particles[1,3] or seeding the growth of ZnO nanowires by solvent methods,[6,11−14] but the products have poor crystallization due to the low growth temperature with the risk of introducing impure ions. The substrates required for epitaxial growth of ZnO nanowires are often expensive, including sapphire,[2,5] GaN,[5,15] and SiC,[16] *etc*. The mass production of high-quality patterned and highly aligned ZnO nanowires at low cost is still a challenge for nanotechnologists. Here, we present a novel route to fabricating high-quality ZnO nanowire arrays with controlled morphology and nanowire density directly from carbonized photoresist (PR) nano/micro-patterns followed by chemical-vapor deposition (CVD).

RESULTS AND DISCUSSION

On a PR-coated Si substrate, large-area and uniformly aligned ZnO nanowire arrays were fabricated by a normal CVD method (Figure 1a,b). To fabricate patterned ZnO nanowires, we first prepared various sizes (from several hundreds of nanometers to several micrometers) and shapes (dot arrays, lines, and networks) of PR patterns on various substrates by photolithography (Figure 1c), and, under a vacuum, these patterns were then annealed and converted to carbonaceous structures that acted as the sites for selective growth of ZnO nanowires (Figure 1d). The sizes, shapes, and numbers of ZnO nanowires formed on one PR pattern can be adjusted by changing the growth conditions. Controlled growth of an individual nanowire at a specific site was demonstrated.

As shown in the optical image in Figure 2a, ZnO nanowire arrays grown on a silicon substrate coated with carbonized PR (1.5 cm × 1.5 cm) had strong absorption of visible light. The high density of ZnO nanowires and their excellent vertical alignment are illustrated in the scanning electron microscope (SEM) image in Figure 2b. These images are very similar to those of high-quality carbon nanotube[17] and nanowire[8] arrays from metal catalytic processes. The nanowires were 20∼200 nm in diameter and 5∼12 μm in length under the growth conditions in this study (see Materials and Methods section) and the size increased with the growth time. In the experiment described here, the PR acted as a buffer layer

*Address correspondence to Phwang@ust.hk.

Received for review August 21, 2008 and accepted December 01, 2008.

Published online December 29, 2008.
10.1021/nn800527m CCC: $40.75

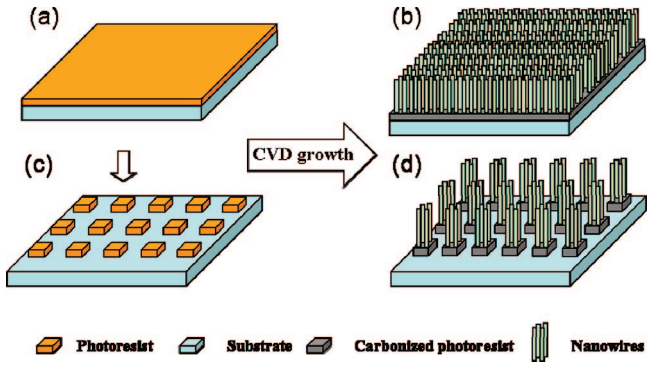

Figure 1. Fabrication process of ZnO nanostructure arrays directly from PR: (a,c) Si substrates coated by PR patterns; (b,d) the resulting nanowire arrays.

between the substrate and the nanowire nuclei to enhance the growth of the aligned ZnO nanowires. The high quality and excellent alignment of the nanowire arrays in a large area is clearly revealed by X-ray diffraction (XRD) images (see Figure 2d). Since the *c*-axes of all ZnO hexagonal nanowires (JCPDS 65-3411) were perpendicular to the substrate, only one strong (0002) diffraction peak was present (Figure 2d, the red curve). Figure 2c shows typical ZnO nanowires grown with the assistance of Au catalysts on a Si substrate under the same growth conditions with diameter and length distributions similar to those with PR. In comparison with the ZnO nanowires fabricated from PR, the poor alignment of the nanowires is clearly reflected by the XRD image as shown in Figure 2d (the green curve) in which

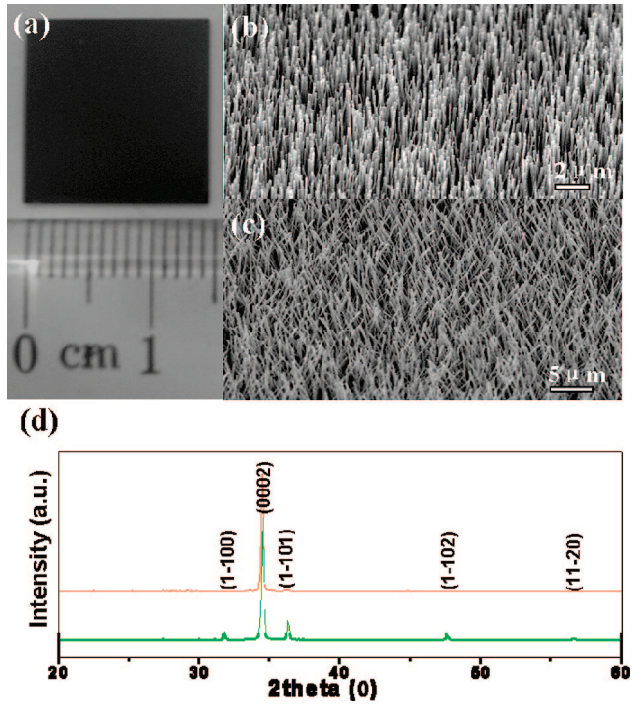

Figure 2. The optical (a) and SEM (b) images of ZnO nanowire arrays grown on a PR-coated silicon substrate; (c) ZnO nanowires formed on an Au-coated silicon substrate; (d) XRD data recorded from the samples shown in panels b (the top curve) and c (the bottom curve).

diffraction peaks at (1-100), (1-101) and (1-102) appear in addition to the (0002) diffraction peak. With the assistance of the PR buffer layer, similar high-quality ZnO nanowire arrays have been obtained on other substrates, such as quartz, Si_3N_4, polycrystalline Al_2O_3, SiC, *etc.* According to our results, the substrates suitable for the present method should be stable at 900 °C and should not react with PR. The simplicity of this method makes it ideal for fast, low-cost and large-area fabrication of high-quality ZnO nanowire arrays.

Figure 3a is a transmission electron microscope (TEM) image showing the typical morphology of nanowires grown along the [0001] direction. When viewed along the [1-100] direction, the thickness contrast profile (see the inset in Figure 3a) indicates the hexagonal shape of the nanowire. The corresponding convergent beam electron diffraction (CBED) pattern (Figure 3b) confirms that the Zn-terminated (0001) planes are the fast growth front. The crystallinity of the nanowires is shown in the high- resolution transmission electron microscope (HRTEM) image in Figure 3c. Our TEM investigation revealed that the fabricated ZnO nanowires contained few defects and were very pure with no impurities detected within the limit of the energy-dispersive X-ray spectrometer (EDX) (Figure 3d). Although point defects, for example, oxygen vacancies and impure atoms, have been long suggested to affect the photoluminance (PL) of ZnO nanocrystals, such defects were not detected by electron microscopy in this study. No good way to determine the defect types and the density qualitatively in nanostructured materials has been established.[18] With a near-field optical microscope (NSOM), we investigated the PL properties of individual ZnO nanowires and found that ZnO nanowires with small diameters (<30 nm) had strong UV emissions without any defect emissions (Figure 3eA), while nanowires with large diameters (>300 nm) always had weak and broad peaks from defect emissions (Figure 3eB). A UV emission at about 380 nm corresponds to the near-band-edge free excitonic emission, while a green-band emission (the defect emission) from 500−550 nm is commonly referred to as a deep-level or trap-state emission.[14] The origin of the deep-level emission is not yet clearly identified, but is generally attributed to point defects such as singly ionized oxygen[19] vacancies and extrinsic impurities.[20] The UV emission peak positions measured from the as-grown ZnO nanowires are diameter-dependent. The position of the PL peaks shifts from 375 (Figure 3eA) to 383 nm (Figure 3eB) as the diameter increases from 30 to 300 nm. The PL spectrum obtained from a large area of the nanowire arrays shows an intense UV emission at 381 nm with a narrow full width at half-maximum (fwhm) of about 15 nm and a weak and broad green emission peak at about 520 nm. These results suggest that the as-grown ZnO nanowires have high crystalline quality. We believe that the high-quality nanowires are fabri-

cated by the growth process described here since no metal catalysts are involved. In addition, we have found that the as-grown samples show excellent antireflection properties, which may have potential applications such as in dielectric antireflection coatings to enhance the efficiency of photovoltaic devices by increasing light coupling in the active region of the devices.[6] We have observed that Si substrates covered by ZnO nanowire arrays have lower reflectance spectra in the range of 350−1100 nm (Figure 3fI and II) and weighted reflectance (R_w) values[21] (11.8% for I and 19.8% for II) compared with random piled ZnO nanowires (Figure 3fV, R_w = 82.5%) and polished Si substrate (Figure 3fVI, R_w = 43.8%). Our samples also show better antireflection response than ZnO nanowire arrays grown from Au catalysts (Figure 3fII). Strong alignment and uniform distribution of ZnO nanowires can enhance the ARCs by effectively trapping light and leading to a broadband suppression in reflection.[6,22] Since the carbonized PR underneath the ZnO nanowires also contributes to the antireflection properties because of its absorption of visible light, we measured the R_w value of the Si substrate coated with the carbonized PR after removing the ZnO nanowires with 10% HNO_3 solution. We measured a low R_w of 26.4% (Figure 3fIII), suggesting that the good ARCs in our samples are the result of the special structure of the aligned ZnO nanowire arrays formed on the carbonized PR.

Compared to other carbon materials, carbonized PRs have remarkable advantages since they can be easily patterned by conventional photolithography. Figure 4 panels a−d illustrate several patterned ZnO nanowire arrays fabricated by our strategy, such as dot arrays (Figures 4a,b), line arrays (Figure 4c), and networks (Figure 4d). The sizes, lengths, and shapes of the ZnO nanowires and their densities in one PR unit can be modified by the growth conditions. As shown in Figure 4e, other morphologies such as ZnO nanopin arrays can be fabricated at a high temperature of 900 °C. Most importantly, our approach has the potential capability to control the number of ZnO nanowires on each PR unit. As demonstrated in Figure 5, we find that the number of ZnO nanowires formed on one pattern decreases as the size of the PR pattern decreases. When the size of the PR pattern is about one micrometer, only a few ZnO nanowires form (see the insets at the bottom of Figure 5a). In Figure 5b, we demonstrate our control of single nanowire growth on a small PR pattern. This growth is achieved by decreasing the evaporation temperature of the ZnO powder to provide a relatively low concentration of Zn to inhibit the excessive nucleation and growth of ZnO nanowires. Notably, these single nanowires are positioned at the corners of the square PR patterns (the dark contrast as marked by the arrows). The formation of one ZnO nucleus on each small PR pattern might be due to the high mobility of the initial Zn catalytic atoms deposited on the PR pattern. Since corners or edges of a patterned structure are often the preferred nucleation sites for material deposition, the catalytic atoms may diffuse preferentially to the corner to form a ZnO nucleus. The density of ZnO nanowire nuclei on the carbonized PR is mainly determined by the substrate temperature, vacuum condition, and source vapor concentration. Once these factors are fixed, the density of the ZnO nanowire nuclei (*i.e.*, the number of ZnO nanowires per unit area) is fixed. Here, when the size of the carbonized PR is small enough, only one ZnO nanowire is formed on each small PR square pattern (Figure 5b).

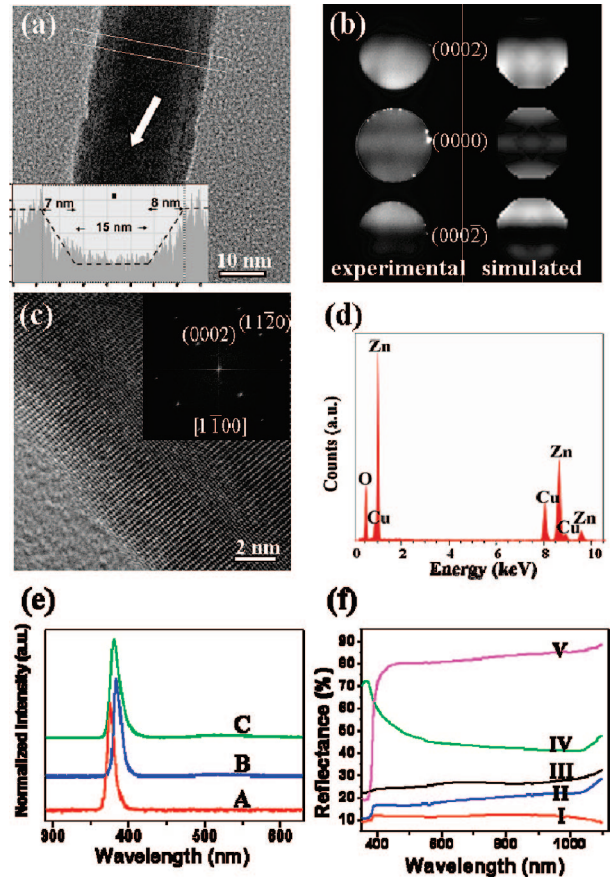

Figure 3. (a) The TEM image of an as-prepared ZnO nanowire and (b) the corresponding CBED patterns viewed along the [1-100] direction (the left one is the experimental result and the right one simulated by JEMS software). (c) An HRTEM image of a ZnO nanowire. The inset is the corresponding Fourier transform pattern. (d) The EDX spectrum recorded from the nanowire shown in panel c. The copper peaks come from the sample supporting the grid. (e) PL spectra from (A) a ZnO nanowire with a diameter of 30 nm; (B) a ZnO nanowire with a diameter of 300 nm and (C) ZnO nanowire arrays. (f) Reflectance spectra of ZnO nanowire arrays grown on (I) PR (Figure 2b), (II) Au-coated silicon substrate (Figure 2c), (III) Si substrate with the remaining carbonized PR after removing the ZnO nanowires with a 10% HNO_3 solution, (IV) naked Si substrate, and (V) random piled ZnO nanowires.

To understand the formation mechanism of ZnO nanowires grown on patterned PR, we used Raman scattering to study the structural changes of the PR layers during the fabrication process. The pristine PR was composed of a photoactive compound called diazonaphthoquinone and novolak. The Raman spectrum

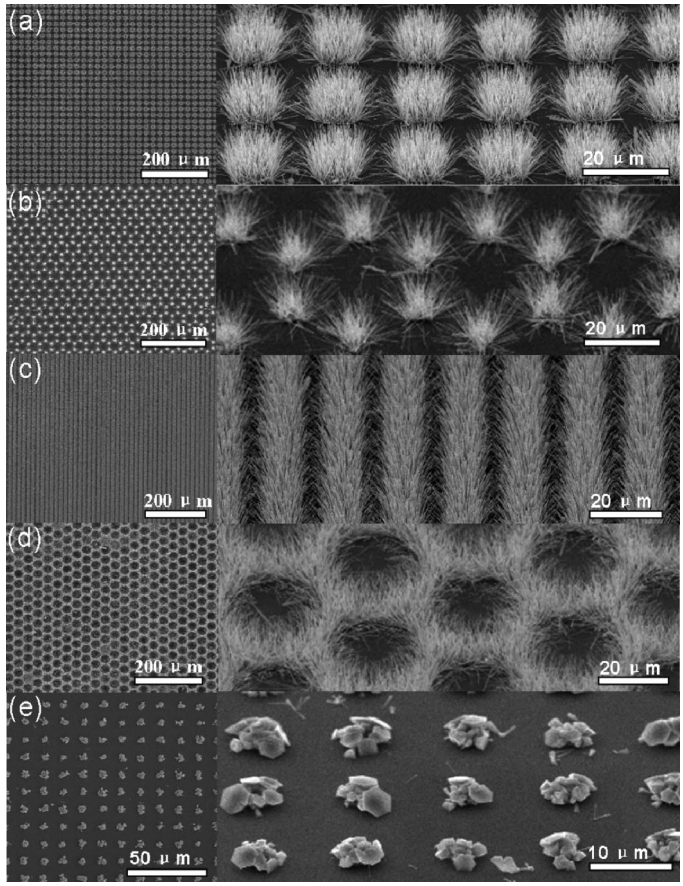

Figure 4. Various ZnO nanostructure arrays from PR patterns: (a) square dot arrays, (b) hexagonal dot arrays, (c) line arrays, (d) hexagonal networks, and (e) ZnO nanopin arrays; on the right side are the corresponding enlarged images.

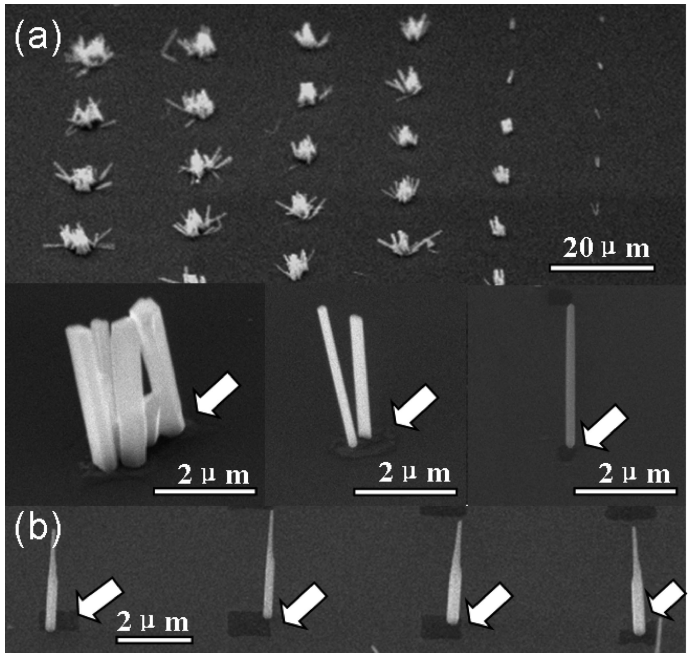

Figure 5. (a) ZnO nanowires grown on different sizes of PR patterns. Insets are enlarged pictures of the ZnO nanowires formed on the patterns. (b) One ZnO nanowire nucleated and grown at the corner of each small PR pattern.

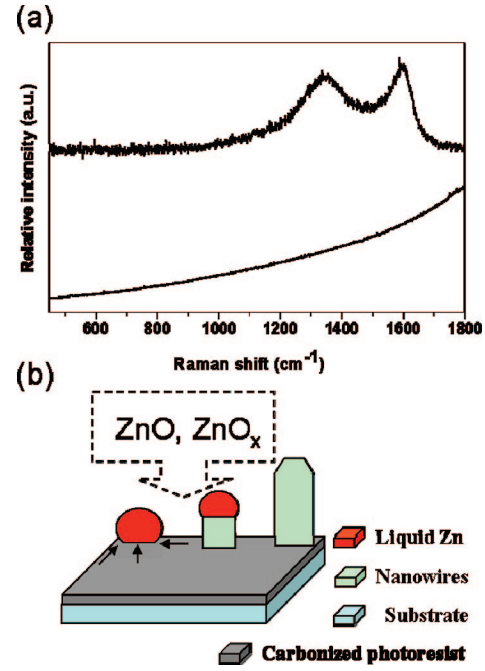

Figure 6. (a) Raman spectra of the photoresists before (the bottom curve) and after annealing (the top curve); (b) nucleation and growth mechanisms of ZnO nanowires on the photoresist patterns.

of the pristine PR showed a uniform background (the bottom curve in Figure 6a) indicating that the pristine PR might contain structures similar to hydrogenated amorphous carbon (a-C:H). After annealing at 800 °C for 30 min, apparent D and G peaks appeared (Figure 6, the top curve). The positions of the D and G peaks were at about 1340 and 1600 cm^{-1}, respectively, which means that carbonaceous materials similar to graphitic structures were formed.[23−26] In the nucleation of ZnO nanowires on carbonized PR, we believed that the carbon plays a critical role since the zinc oxide vapor phase evaporated from the solid source could easily react with carbon[27] at a high temperature, and Zn could be extracted to form Zn droplets by the following reactions (Figure 6b):

$$2ZnO(g) + C(s) \leftrightarrow 2Zn(l) + CO_2(g) \quad (1)$$

or

$$2ZnO_x(g) + xC(s) \leftrightarrow 2Zn(l) + xCO_2(g) \quad (2)$$

Since the melting temperature of Zn is much lower than that of ZnO, Zn droplets form preferentially on the carbonized PR layer and act as catalysts for ZnO nanowire growth as suggested in refs 28 and 29. That reactions 1 and 2 require a high temperature and Zn vaporizes above 907 °C means that our growth temperature is in the range 700∼900 °C. Although the presence of impure nanoparticles or capped Zn particles at the tips of nanowires has been regarded as one of the characteristics of VLS growth, our HRTEM investigation (Fig-

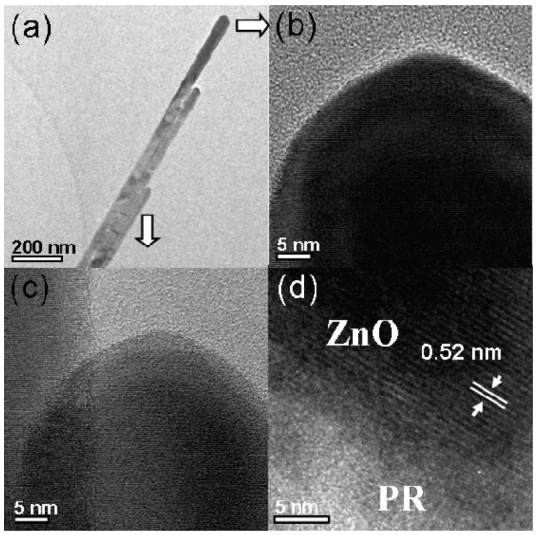

Figure 7. (a) TEM images of the tips of ZnO nanowire; (b,c) HRTEM images of the tips; (d) cross-section TEM image of the interface between the root of the ZnO nanowire and the PR.

ure 7a−c) reveals that there are no capped nanoparticles at the tips of the as-synthesized ZnO nanowires.

The interface between the root of a ZnO nanowire and the PR was investigated by cross-sectional HRTEM imaging (see Figure 7d). The carbonized PR is an amorphous-like structure and the ZnO crystal is found to nucleate on this flat PR layer with its (0001) planes parallel to the PR surface. The formation mechanism of the oriented ZnO nanowire nuclei on the PR layer remains unknown. However, the present results show a similarity with some recent theoretical and experimental works[28,30,31] that the (0001)-oriented ZnO films or nanowire arrays (evolved from an initial hexagonal BN-like nucleating layer) are preferentially formed on flat substrates such as silicon and Ag by pulsed laser deposition methods. In this case, there is no orientation relationship between ZnO crystals and the substrates except that the ZnO (0001) planes are parallel to the substrate surface. The ZnO nanowire arrays formed on the PR layers have a very similar growth behavior. Under the present growth conditions, carbonized PR not only provides perfect nucleation sites for the growth of aligned ZnO nanowires, but it also forms excellent electrodes that connect to the nanowires. After further annealing, the resistivity of the PR patterns was determined to be about $1 \times 10^{-3}\ \Omega \cdot$cm, which is comparable to that of indium tin oxide ($10^{-3}-10^{-5}\ \Omega \cdot$cm).[32] These electrodes have excellent biocompatibility, chemical inertness, good thermal conductivity, and thermal and mechanical stability and therefore are ideal for many nanomaterial applications.[24] Moreover, the high-quality ZnO nanowire arrays with desired patterns fabricated by this simple and low-cost method also have great potential applications in two-dimensional photonic crystals,[33] nano-optoelectronics, nanosensors arrays,[34] and UV photovoltaic cells,[35] *etc.*

CONCLUSIONS

We have demonstrated a simple and effective method for fabricating and patterning high-quality ZnO nanowire arrays with controlled nucleation sites and densities on carbonized PRs. ZnO nanowires nucleate preferentially on the carbonized PR patterns, which are also excellent electrodes for connecting to ZnO nanostructures. ZnO nanowires grown directly from PRs show excellent crystal quality, stability, strong UV emissions, and excellent antireflection performance to visible light with a low R_w.

MATERIALS AND METHODS

Preparation of PR patterns: Si substrates (1.5 cm × 1.5 cm) were coated with a thin layer of PR (photoresist AZ1518, HPR204, or SPR6112) by spin coating at a speed of 4000 rpm for 30 s and then treated by hard-baking at 120 °C for 60 s. The patterned PRs were made using an ABM contact aligner. The exposure time was set to 4.3 s and the developing time was 60 s.

Growth of ZnO nanowire arrays: An alumina boat containing 3 g of ZnO powder was placed in the center of a tube furnace. Si substrates with PR patterns were placed downstream for the nucleation and growth of ZnO nanowires. The furnace was heated to 1300 °C and kept for half an hour under vacuum conditions (~10^{-2} Torr). ZnO nanowires were found to grow on the substrates when the temperature was about 700~900 °C. For the growth of the nanowires shown in Figure 5b, the growth temperature was decreased to 1200 °C to provide a relatively low concentration of Zn in order to inhibit the excessive nucleation and growth of the ZnO nanowires.

The as-grown nanowires were characterized by a Philips scanning electron microscope (SEM, XL-30) and a JEOL high-resolution transmission electron microscope (HRTEM, 2010F) equipped with an energy-dispersive X-ray spectrometer (EDX). Convergent-beam electron diffraction (CBED) measurement was carried out on a Philips TEM (CM120) at 80 kV for optimal contrast. Photoluminescence (PL) measurement of individual nanowires was conducted using a near-field optical microscope (NSOM, Nanonics Cryoview2000) equipped with a He−Cd laser (325 nm). The Raman spectra were measured at room temperature using a Jobin Yvon-T64000 micro-Raman spectrometer (Ar laser excitation at 514.5 nm).

Acknowledgment. We thank Baikui Li, T. K. Zhang, and W.Y. Law for their technical assistance in the preparation of metal electrodes for the electrical measurements. We are grateful to Y. J. Lee of Sandia National Laboratories, Albuquerque, NM, for helpful discussions and for suggesting a method for the calculation of R_w. This work was financially supported by the Research Grants Council of Hong Kong (Project Nos. N_HKUST615/06, 602305, and 603006).

REFERENCES AND NOTES

1. Lee, S. W.; Jeong, M. C.; Myoung, J. M. Magnetic Alignment of ZnO Nanowires for Optoelectronic Device Applications. *Appl. Phys. Lett.* **2007**, *90*, 133115-1–133115-3.
2. Wang, X. D.; Zhou, J.; Song, J. H.; Liu, J.; Xu, N.; Wang, Z. L. Piezoelectric Field Effect Transistor and Nanoforce Sensor Based on a Single ZnO Nanowire. *Nano Lett.* **2006**, *6*, 2768–2772.

3. Zimmler, M. A.; Stichtenoth, D.; Ronning, C.; Yi, W.; Narayanamurti, V.; Voss, T.; Capasso, F. Scalable Fabrication of Nanowire Photonic and Electronic Circuits Using Spin-On Glass. *Nano Lett.* **2008**, *8*, 1695–1699.
4. Yang, P.; Yan, H.; Mao, S.; Russo, R.; Johnson, J; Saykally, R.; Morris, N.; Pham, J.; He, R.; Choi, H. J. Controlled Growth of ZnO Nanowires and Their Optical Properties. *Adv. Fun. Mater.* **2002**, *12*, 323–331.
5. Wang, X. D.; Song, J. H.; Liu, J.; Wang, Z. L. Direct-Current Nanogenerator Driven by Ultrasonic Waves. *Science* **2007**, *316*, 102–105.
6. Lee, Y. J.; Ruby, D. S.; Peters, D. W.; McKenzie, B. B.; Hsu, J. W. P. ZnO Nanostructures as Efficient Antireflection Layers in Solar Cells. *Nano Lett.* **2008**, *8*, 1501–1505.
7. Sun, X. W.; Wang, J. X. Fast Switching Electrochromic Display Using a Viologen-Modified ZnO Nanowire Array Electrode. *Nano Lett.* **2008**, *8*, 1884–1889.
8. Fan, H. J.; Werner, P.; Zacharias, M. Semiconductor Nanowires: From Self-Organization to Patterned Growth. *Small* **2006**, *2*, 700–717.
9. Collins, C. B.; Carlson, R. O.; Gallagher, C. Properties of Gold-Doped Silicon. *Phys. Rev.* **1957**, *105*, 1168–1173.
10. Oh, S. H.; van Benthem, K.; Molina, S. I.; Borisevich, A. Y.; Luo, W.; Werner, P.; Zakharov, N. D.; Kumar, D.; Pantelides, S. T.; Pennycook, S. J. Point Defect Configurations of Supersaturated Au Atoms Inside Si Nanowires. *Nano Lett.* **2008**, *8*, 1016–1019.
11. Greene, L.; Law, M.; Tan, D. H.; Goldberger, J.; Yang, P. General Route to Vertical ZnO Nanowire Arrays Using Textured ZnO Seeds. *Nano Lett.* **2005**, *5*, 1231–1236.
12. Wu, J. J.; Liu, S. C. Low-Temperature Growth of Well-Aligned ZnO Nanorods by Chemical Vapor Deposition. *Adv. Mater.* **2002**, *14*, 215–218.
13. Choy, J. H.; Jang, E. S.; Won, J. H.; Chung, J. H.; Jan, D. J.; Kim, Y. W. Soft Solution Route to Directionally Grown ZnO Nanorod Arrays on Si Wafer; Room-Temperature Ultraviolet Laser. *Adv. Mater.* **2003**, *15*, 1911–1914.
14. Tam, K. H.; Cheung, C. K.; Leung, Y. H.; Djurii, A. B.; Ling, C. C.; Beling, C. D.; Fung, S.; Kwok, W. M.; Chan, W. K.; Phillips, D. L.; *et al.* Defects in ZnO Nanorods Prepared by a Hydrothermal Method. *J. Phys. Chem. B* **2006**, *110*, 20865–20871.
15. Fan, H. J.; Fleischer, F.; Lee, W.; Nielsch, K.; Scholz, R.; Zacharias, M.; Gösele, U.; Dadgar, A.; Krost, A. Patterned Growth of Aligned ZnO Nanowire Arrays on Sapphire and GaN layers. *Superlattices Microstruct.* **2004**, *36*, 95–105.
16. Ng, H. T.; Han, J.; Yamada, T.; Nguyen, P.; Chen, Y. P.; Meyyappan, M. Single Crystal Nanowire Vertical Surround-Gate Field-Effect Transistor. *Nano Lett.* **2004**, *4*, 1247–1252.
17. Yan, Y; Chan-Park, M. B.; Zhang, Q. Advances in Carbon-Nanotube Assembly. *Small* **2006**, *3*, 24–42.
18. Djurisic, A. B.; Leung, Y. H. Optical Properties of ZnO Nanostructures. *Small* **2006**, *2*, 944–961.
19. Vanheusden, K.; Warren, W. L.; Seager, C. H.; Tallant, D. R.; Voigt, J. A.; Gnade, B. E. Mechanisms Behind Green Photoluminescence in ZnO Phosphor Powders. *J. Appl. Phys.* **1996**, *79*, 7983–7990.
20. Dingle, R. Luminescent Transitions Associated With Divalent Copper Impurities and the Green Emission from Semiconducting Zinc Oxide. *Phys. Rev. Lett.* **1969**, *23*, 579–581.
21. Weighted reflectance R_w was calculated by normalizing the reflectance spectra with the internal quantum efficiency spectra of a typical multicrystalline Si solar cell and the terrestrial global solar spectrum (AM1.5). For detailed calculation process, please refer to ref 6. Absolute hemispherical reflectance measurements were carried out with a UV−vis spectrophotometer (Lambda 20) and an integrating sphere (Labsphere) with a sampling spot of 10 mm × 10 mm at normal incidence.
22. Lee, C.; Bae, S. Y.; Mobasser, S.; Manohara, H. A Novel Silicon Nanotips Antireflection Surface for the Micro Sun Sensor. *Nano Lett.* **2005**, *5*, 2438–2442.
23. Li, Y.; Lee, E. J.; Cai, W. P.; Kim, K. Y.; Sung, O. C. Unconventional Method for Morphology-Controlled Carbonaceous Nanoarrays Based on Electron Irradiation of a Polystyrene Colloidal Monolayer. *ACS Nano* **2008**, *2*, 1108–1112.
24. Park, B. Y.; Taherabadi, L.; Wang, C.; Zoval, J.; Madou, M. J. Electrical Properties and Shrinkage of Carbonized Photoresist Films and the Implications for Carbon Microelectromechanical Systems Devices in Conductive Media. *J. Electro.Chem. Soc.* **2005**, *152*, J136–J143.
25. Takashi, K.; Toshiki, M.; Akira, T. Formation of a Flexible Graphite Film from Poly(acrylonitrile) Using a Layered Clay Film as Template. *Chem. Mater.* **1994**, *6*, 2138–2142.
26. Miao, J. Y.; Cai, Y.; Chan, Y. F.; Sheng, P.; Wang, N. A Novel Carbon Nanotube Structure Formed in Ultra-Long Nanochannels of Anodic Aluminum Oxide Templates. *J. Phys. Chem. B* **2006**, *110*, 2080–2083.
27. Yao, B. D.; Chan, Y. F.; Wang, N. Formation of ZnO Nanostructures by a Simple Way of Thermal Evaporation. *Appl. Phys. Lett.* **2002**, *81*, 757–759.
28. Sun, Y.; Fuge, G. M.; Ashfold, M. N. R. Growth of Aligned ZnO Nanorod Arrays by Catalyst-Free Pulsed Laser Deposition Methods. *Chem. Phys. Lett.* **2004**, *396*, 21–26.
29. Wei, Y.; Ding, Y.; Li, C.; Xu, S.; Ryo, J.; Dupuis, R.; Sood, A. K.; Polla, D. L.; Wang, Z. L. Growth of Vertically Aligned ZnO Nanobelt Arrays on GaN Substrate. *J. Phys. Chem. C*, , . in press.
30. Claeyssens, F.; Freeman, C. L.; Allan, N. L.; Sun, Y.; Ashfold, M. N. R.; Harding, J. H. Growth of ZnO Thin Films−Experiment and Theory. *J. Mater. Chem.* **2005**, *15*, 139–148.
31. Tusche, C.; Meyerheim, H. L.; Kirschner, J. Obervation of Depolarized ZnO (0001) Monolayers: Formation of Unreconstructed Planar Sheets. *Phys. Rev. Lett.* **2007**, *99*, 026102-1–026102-4.
32. Weng, X. L.; Tang, W.; Wu, Y. T.; Deng, L. J. Microstructure and Resistivity of Low Temperature Deposition ITO Films on PET Substrate by Magnetron Sputtering. *Key Eng. Mater.* **2007**, *353*, 1867–1870.
33. Wang, X. D.; Neff, C.; Graugnard, E.; Ding, Y.; King, J. S.; Pranger, L. A.; Tannenbaum, R.; Wang, Z. L.; Summers, C. J. Photonic Crystals Fabricated Using Patterned Nanorod Arrays. *Adv. Mater.* **2005**, *17*, 2103–2106.
34. Wang, X. D.; Summers, C. J.; Wang, Z. L. Large-Scale Hexagonal-Patterned Growth of Aligned ZnO Nanorods for Nano-Optoelectronics and Nanosensor Arrays. *Nano Lett.* **2004**, *4*, 423–426.
35. Cole, J. J.; Wang, X.; Knuesel, R. J.; Jacobs, H. O. Integration of ZnO Microcrystals with Tailored Dimensions Forming Light Emitting Diodes and UV Photovoltaic Cells. *Nano Lett.* **2008**, *8*, 1477–1481.